Behavioural Brain Research 394 (2020) 112834

Contents lists available at ScienceDirect

Behavioural Brain Research

journal homepage: www.elsevier.com/locate/bbr

Intermittent theta burst stimulation over the dorsomedial prefrontal cortex modulates resting-state connectivity in depressive patients: A sham-controlled study

J. Persson[a,*], W. Struckmann[a], M. Gingnell[a,c], D. Fällmar[b], R. Bodén[a]

[a] Department of Neuroscience, Psychiatry, Uppsala University, Uppsala, Sweden
[b] Department of Surgical Sciences, Radiology, Uppsala University, Uppsala, Sweden
[c] Department of Psychology, Uppsala University, Uppsala, Sweden

ARTICLE INFO

Keywords:
iTBS
dmPFC
sgACC
Depression
Resting-state
fMRI

ABSTRACT

The mechanisms underlying repetitive transcranial magnetic stimulation (rTMS) treatment are largely unknown. Although there is a general lack of sham controlled studies, findings show altered functional connectivity to the stimulated region following treatment. When targeting the dorsolateral prefrontal cortex (dlPFC), connectivity with the subgenual anterior cingulate cortex (sgACC) is predictive of response, but less is known about the effects on functional connectivity of targeting the dorsomedial PFC (dmPFC). Here, 30 patients with an ongoing depressive episode were recruited and randomized to 20 sessions at target intensity of either active or sham intermittent theta burst stimulation (iTBS) over dmPFC. Those receiving sham were offered active treatment in a subsequent open phase. A seven minute resting-state scan and depressive symptom assessment was performed before and after treatment. After exclusions due to attrition and excessive head movements 23 patients remained for analysis. Seed-based resting-state connectivity was calculated using two seeds for the dmPFC target as well as the sgACC. A symptom related increase in dmPFC connectivity after active treatment, compared to sham treatment, was found. The effect was observed in a region overlapping the precuneus and the posterior cingulate cortex (PCC), suggesting an increase in the connectivity between the targeted salience network and the default mode network mediating improvement in depressive symptoms. Connectivity between the precuneus and both the sgACC and the treatment target was predictive of symptom improvement following active treatment. The findings have implications for understanding the mechanisms behind iTBS and may inform future efforts to individualize the treatment.

1. Introduction

Repetitive transcranial magnetic stimulation (rTMS) is an emerging treatment option for treatment resistant depression, with meta-analyses of randomized sham-controlled trials supporting its efficacy and tolerability [1,2]. While the established treatment protocol entails pulse trains at 10 Hz delivered over the left dorsolateral prefrontal cortex (dlPFC) or at 1 Hz over the right dlPFC, optimal treatment parameters are yet to be determined. Recently, intermittent theta burst stimulation (iTBS) was shown to be comparable in efficacy to the standard 10 Hz protocol with similar dropout rates, while greatly reducing the duration of each treatment session [3]. Additionally, studies have found that multiple daily iTBS sessions, given with at least 15 min intervals, increase cortical excitability compared to a single session [4,5], with some suggestion that this may lead to shortened time to treatment response [6]. Alternative prefrontal treatment targets have also been evaluated with the dorsomedial PFC (dmPFC) showing promising results in an open label study [7] and in a sham-controlled trial [8]. The rationale for targeting this region is based on converging findings pointing to a more central role of dmPFC in emotion regulation compared to the dlPFC as well as the observation that dmPFC shows aberrant connectivity with major resting-state networks in major depression [9,10]. Resting state functional magnetic resonance imaging (rs-fMRI) is well suited for assessing modulation of widespread functional networks affected in depression following rTMS, by measuring changes in whole-brain functional connectivity. Earlier studies using this approach in dlPFC targeted treatment have found that baseline connectivity between the striatum or insula and the dlPFC was predictive of treatment response [11–13]. Similarly, salience network (SN) centrality, a graph theoretical measure, also predicted response to

* Corresponding author at: Psychiatry, Uppsala University Hospital, 751 85, Uppsala, Sweden.
E-mail address: jonas.persson@neuro.uu.se (J. Persson).

https://doi.org/10.1016/j.bbr.2020.112834
Received 2 April 2020; Received in revised form 21 July 2020; Accepted 22 July 2020
Available online 26 July 2020

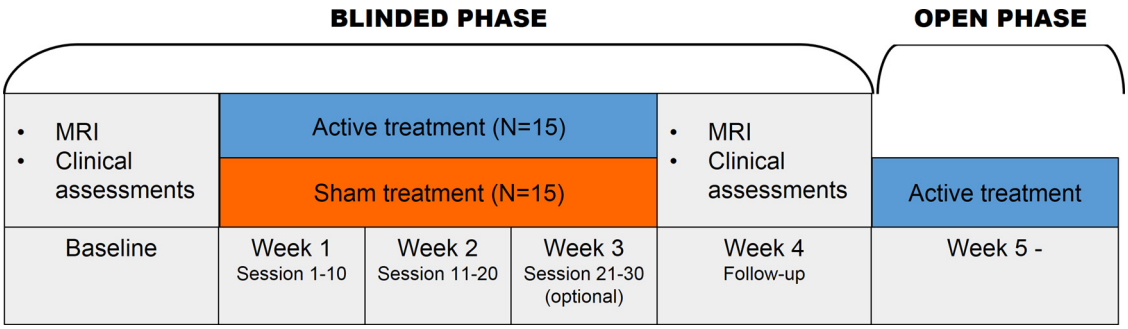

Fig. 1. An overview of the study design, detailing the assessments relative to treatment, duration of sham-controlled treatment and the interval between blinded and open phase treatment.

dlPFC treatment [14]. Changes in dlPFC connectivity have been observed following dlPFC-targeted treatment in open label [15] as well as sham controlled [16] studies. Regarding dmPFC targeted treatment, baseline connectivity with the ventromedial PFC separated responders from non-responders using a graph theory based approach [17] while seed-based connectivity with dmPFC predicted treatment [18]. Findings also suggest a central role for the subgenual anterior cingulate cortex (sgACC) in mediating treatment response to rTMS over both dlPFC [15,19–22] and dmPFC [18].

Notably, there is a lack of controlled studies on the modulation of functional connectivity following rTMS treatment of depressive symptoms. This leaves open the possibility that the findings summarized above partly reflect non-specific treatment effects. Thus, while earlier findings suggest that rTMS targets functional networks via a cortical node and acts by modulating these networks, only one study has actually demonstrated a treatment specific modulation of functional connectivity in a sham controlled setting following a full dlPFC treatment [16]. No study to date has considered such mechanisms underlying dmPFC-targeted treatment in a sham controlled study.

Here, rs-fMRI was measured before and after 20 sessions at target intensity of active or sham iTBS over dmPFC to see whether active treatment modulates connectivity to the dorsomedial target as well as the sgACC, compared to sham treatment, and whether this is related to improvement in depressive symptoms. A further aim was to investigate whether dmPFC or sgACC connectivity at baseline is predictive of treatment response.

2. Methods and materials

2.1. Participants

This project shares data with a randomized controlled trial (RCT; NCT02905604), with 30 out of 40 patients with depression who additionally underwent brain imaging before and after treatment. While the results from the RCT are yet to be reported, patients have been continuously unblinded according to the protocol and the primary outcome measure is not reported here.

Thirty patients were recruited from the psychiatric outpatient clinic at the Uppsala University Hospital, Sweden. The patients, of which three were diagnosed with bipolar disorder, all met criteria for an ongoing depressive episode as verified through a Mini International Neuropsychiatric Interview (M.I.N.I.) [23]. We included patients with bipolar depression as well, since large meta-analyses did not find any difference in response or remission rates to rTMS over dlPFC, compared to unipolar depression [1,2] and since bipolar depression is similarly associated with decreased metabolism and grey matter density in dlPFC and dmPFC [24,25]. Indeed, this transdiagnostic approach may be preferable both with regards to symptom dimensions [26,27] and the underlying connectome [28,29]. To be eligible for inclusion, patients had to be between 18 and 59 years of age with unchanged medication the past month. Contraindications included epilepsy, metal implants, active substance use disorder, and pregnancy. Written informed consent was obtained from all participants. One patient in the active arm dropped out during treatment and was not available for follow-up assessments. Due to excessive head movements (see preprocessing below for details) three patients in each arm were excluded.

The study was approved by the Research Ethical Review Board, Uppsala.

2.2. Study design and procedures

The patients were block-randomized with block sizes 6 and 8 in random order to either active or sham treatment. Pretreatment assessments included self-assessed depressive symptom ratings using the Montgomery Åsberg Depression Rating Scale (MADRS-S) [30] and magnetic resonance imaging (MRI). Treatment with iTBS was started on the nearest following weekday and continued for between 10 and 15 consecutive weekdays, until 10 days of treatment at full intensity was achieved. This was done in order to increase tolerability according to the protocol specified below. Posttreatment assessments were performed four weeks after the pretreatment assessment, regardless of the number of treatment days, and after this the treatment was unblinded. From end of stimulation to posttreatment assessments (9–16 days) no medication changes or other treatments were initiated. Patients having received sham treatment without responding, defined as a 25 % symptom reduction, were then offered active treatment with the same protocol. Fig. 1 gives a graphical overview of the study design.

2.3. Transcranial magnetic stimulation

The treatment protocol consisted of neuronavigated iTBS over dmPFC, using individual anatomical images acquired during the pretreatment scanning session and targeting the dorsal anterior cingulate cortex (dACC), Montreal Neurological Institute (MNI) coordinates: X = 0, Y = 30, Z = 30 [31]. Neuronavigation was accomplished using the Localite TMS Navigator from Localite, Bonn, Germany. For the treatment to plausibly reach this deeper lying region, the stimulation intensity was based on the foot, rather than hand, motor threshold. The stimulation intensity was set to 90 % of the motor threshold. Treatment was delivered with the stimulator MagPro X100 with MagOption using the Cool D-B80 A/P coil from MagVenture, Farum, Denmark. This coil is designed for deep stimulation and built for use in sham controlled studies. It consists of two 120° angled figure-of-eight coils back-to-back, one of them shielded for sham stimulation. Each patient was randomized to a code that, when entered into the stimulator, decided which side of the coil is to be used. Transcutaneous electrical nerve stimulation (TENS) electrodes were fitted to the forehead directly beneath the center of the coil, and during sham stimulation delivered current synchronized to the TMS pulses in order to mimic the sensation of active stimulation. The coil was placed over the forehead, with the handle pointing to the patient's left. During each treatment day, two sessions of

iTBS were delivered, interspersed by a pause of 15 min, since a previous study showed that twice daily iTBS with a 15 min interval facilitated the motor response to single pulses, compared to a single session or two sessions with a shorter interval [4]. Each session consisted of 40 pulse trains of biphasic pulses for a total of 1200 pulses. Halfway through each session, the pulses were reversed, resulting in 20 pulse trains with the initial current direction going left-to-right and 20 pulse trains right-to-left. This was done in order to achieve bilateral stimulation of the dmPFC, according to a previously published protocol [7]. Treatment was delivered at target intensity for 20 twice daily sessions corresponding to 10 week days [7]. To increase tolerability, the stimulation intensity was gradually increased during the initial treatment sessions, based on pain ratings from the patient, until target stimulation intensity was reached. If the target intensity was not reached for at least 50 % of the delivered trains on a treatment day, an additional treatment day was added, for up to 15 days in total. During treatment, daily assessments of adverse effects were conducted.

2.4. Magnetic resonance imaging

MRI data was collected on a 3 T scanner (Philips Achieva, Philips Medical Systems, Best, Netherlands), using a 32-channel head coil. T1-weighted structural imaging was performed using a 3D Turbo Spin Echo sequence, with TR/TE = 8.2/3.8 ms, flip angle = 8°; field of view = 256 × 256 mm^2; voxel size = 1 × 1 × 1mm^3 isotropic voxels; 220 slices.

Functional MRI (fMRI) data were acquired with eyes open, during a seven minute scan. A white fixation cross was presented over black background using MRI compatible goggles from Nordic NeuroLab, attached to the head coil. Functional imaging consisted of single-shot gradient echo-planar imaging with interleaved acquisition, 32 slices, TR/TE = 2000/30 ms, field of view (FOV) = 192 × 192mm^2, voxel size = 3 × 3 × 3mm^3 isotropic voxels.

2.5. Preprocessing of resting state data

Preprocessing was performed in DPABI [32] and analyses were run in Statistical Parametric Mapping 12 (SPM12), using MATLAB R2017b. After removing the first four volumes, slice-time corrected functional images were realigned to compensate for head movement during image acquisition. 24 nuisance regressors were defined based on the realignment parameters to model out movement related noise and consisted of six head motion parameters, the six corresponding parameters from the preceding time point, and their respective squared counterparts [33]. To further account for excessive head movement, frame-wise displacement (FD) was calculated according to Jenkinson et al. [34]. Volumes with a corresponding FD > .25 were regressed out. If less than four minutes of data remained after this procedure, the participant was excluded [35]. In this way, 11 patients receiving active treatment and 12 patients receiving sham treatment remained. In these remaining patients, 185.2 ± 22.5 out of 206 volumes were retained on average. In addition, mean time series from white matter and cerebrospinal fluid were regressed out.

Structural T1-weighted images were segmented using the algorithm in SPM12 and Diffeomorphic Anatomical Registration Through Exponentiated Lie Algebra (DARTEL) was used to create a study specific template for improved normalization. The resulting parameters were applied to the residual functional images, after coregistering them to the structural image, in order to bring them into MNI space. Spatial smoothing was applied to the warped images with a Gaussian kernel of 6 mm full width at half maximum (FWHM).

2.6. Resting state connectivity

Seed-based connectivity was used to assess whole-brain connectivity with the dmPFC treatment target. The same MNI coordinates earlier used for neuronavigation of the treatment target (X = 0, Y = 30, Z = 30) defined the center of a spherical region of interest (ROI) with a radius of 10 mm to overlap with bilateral gray matter (see Supplemental Fig. 1, red mask). Connectivity to this region has been found to be modulated by dmPFC rTMS in an open-label study [18]. Additionally, since previous studies suggest that the sgACC mediates response to rTMS [15,18–21] an additional sgACC seed ROI was based on the bilateral cingulate region mask from the IBASPM 71 atlas provided with the WFU PickAtlas Toolbox. Voxels within the mask ventral to the axial slice bisecting the genu, and posterior to the most anterior coronal slice containing the genu, were retained. To account for signal drop-out in this region, only voxels within the remaining ROI where all participants contributed signal from both the pre- and post-treatment scanning were retained (see Supplemental Fig. 1, blue mask, and Supplementary material for details on signal quality within the retained portion of the sgACC ROI). A temporal bandpass filter was applied to the functional images by multiplying the signal with a rectangular function in the frequency domain, with cutoff frequencies of 0.01 and 0.1 Hz, after which voxel-wise correlations using the mean signal from each ROI were calculated for each individual and scanning session (pre- and post-treatment). The resulting voxel-wise correlation coefficients were transformed using Fisher r-to-z-transformation. Finally, voxel-wise subtraction of the transformed correlation maps from the pre-treatment session from the post-treatment maps was done to obtain difference maps reflecting connectivity changes after treatment.

2.7. Statistical procedures

In order to assess changes in connectivity with each seed region after active compared to sham treatment, two-sample pseudo t-tests were run in SPM12 using the Statistical nonparametric Mapping 13 (SnPM13) toolbox [36], contrasting the difference maps between the two groups.

Further, to assess different mechanisms of symptom improvement in active compared to sham treatment, an interaction term between MADRS-S delta-scores (calculated by subtracting follow-up from baseline scores) and treatment group was added as a covariate of interest, together with MADRS-S delta-scores and group as separate covariates, to model the interaction between treatment and symptom change. Here, to follow up on significant findings, separate contrasts were specified to test for the relationship between connectivity change and symptom change within each group. For the above models, additional ROI based analyses were performed with the treatment target or sgACC seeds to test for modulation of the connectivity between these two regions following treatment. Age and treatment days received were added as nuisance covariates in all models.

Finally, a separate analysis was conducted to assess any connectivity at baseline predictive of treatment response. As participants partaking in the sham-treatment were later offered active treatment, connectivity maps from the pre-treatment session in the active group and the post-treatment session in the sham group (acquired just before the start of active treatment) were combined and analyzed together, specifying a regressor containing MADRS-S delta-scores during active treatment and group (blind or open phase) as a nuisance regressor.

P-values were estimated using 5000 permutations. Voxels surviving a cluster-level corrected threshold of $p < .05$, using a cluster forming threshold of $p < .001$, were considered significant.

3. Results

Demographic and clinical baseline description of the study sample is presented in Table 1. The treatment groups were of similar composition at baseline. The change in MADRS-S score (baseline - follow-up) was 6.3 ± 9.1 for the active treatment and 3.8 ± 6.2 for the sham treatment. A repeated measures ANOVA showed no significant group (active vs. sham) × time (pre- vs. post-treatment) interaction, $F(1,21) = .57$, p

Table 1
Demographical variables and symptom ratings, presented separately for those receiving active versus sham treatment. Significance tests are also presented, assessing the difference between the two groups for each variable. MADRS-S: Montgomery-Åsberg Depression Rating Scale, self-report; EQ VAS: Visual Analogue Scale self-rated health from EQ-5D; MSM: Maudsley Staging Method for treatment resistant depression.

	Active (n = 11)	Sham (n = 12)	Test for difference
Years of age, mean (sd)	32.2 (11.4)	25.8 (6)	$t(21) = -1.72$, p = .100
Gender, male:female	5:6	6:6	X^2 = .048, p = .827
MADRS-S pre-treatment, mean (sd)	29.7 (6.2)	28 (8.4)	$t(21) = -.56$, p = .583
EQ VAS, mean (sd)	31.6 (14.9)	36.7 (13.9)	$t(21)$ = .85, p = .402
MSM-total, mean (sd)	9.9 (1.8)	10.4 (2)	$t(21)$ = .65, p = .524
Education, n			
9th year completed	0	4	
12th year completed	6	5	
Higher education	5	3	
Primary diagnosis, n			
Depressive episode	5	8	
Recurrent depression	5	3	
Bipolar disorder	1	1	
Secondary diagnoses, n*			
Anxiety disorders	7	9	
Obsessive-compulsive disorder	1	0	
Post-traumatic stress disorder	1	2	
Attention deficit (and hyperactivity) disorder	2	4	
Autism spectrum disorder	1	0	
Personality disorder	0	2	
Medication, n			
Antidepressants	9	9	
Lithium	2	1	
Lamotrigine	2	0	
Second generation antipsychotics	2	3	
Stimulants	0	4	
No mood medication	3	0	

* note that one patient can have more than one secondary diagnosis.

= .459, but a significant main effect of time, F(1,21) = 9.79, p = .005, reflecting a general symptom improvement regardless of treatment.

Seven patients receiving active, and 2 patients receiving sham, treatment underwent more than 10 days of treatment due to not reaching target intensity during the first few sessions. A Welch *t*-test showed a significant difference in treatment days received, $t(21) = -3.05$, p = .011, 12.5 ± 2.4 days and 10.2 ± .6 days in the active and sham groups, respectively. This was included as a nuisance covariate in the following analyses.

3.1. Changes in connectivity strength following active versus sham iTBS

There were no significant differences in whole-brain connectivity change with the treatment target between the active and sham conditions. The same was true for sgACC connectivity change and for the ROI based analyses.

3.2. Symptom related changes in connectivity following active versus sham iTBS

A region peaking in the posterior precuneus showed a relationship between change in connectivity to the treatment target and MADRS-S change after active compared to sham treatment (peak coordinates: X = 21, Y = -60, Z = 21, t(18) = 4.97, cluster extent = 35, cluster-level corrected p = .048). This precuneus cluster bordered on the cuneus and extended into the posterior cingulate cortex (PCC), see Fig. 2. To further investigate what was driving this interaction, separate analyses were run for each group, correlating connectivity change to MADRS-S change. This showed a positive relationship in the active group in the same region (peak coordinates: X = 21, Y = -60, Z = 21, t(9) = 7.29, cluster extent = 16, cluster-level corrected p = .013), with no significant correlation in the sham group. In other words, the greater the symptom improvement following active treatment, the more the connectivity between the treatment target and the right posterior precuneus moved in the positive direction. No symptom related change in sgACC connectivity was found, or in treatment target connectivity when using sgACC as a ROI.

3.3. Connectivity predictive of symptom improvement after active iTBS

Of the 12 patients receiving sham treatment, nine underwent active treatment in a subsequent open phase, lending 20 patients available for correlating pretreatment connectivity to MADRS-S change. Regarding connectivity to the treatment target, a significant effect was found, reflecting a negative relationship between baseline connectivity and MADRS-S change within the right cuneus (peak coordinates: X = 9, Y = -69, Z = -9, T(17) = 7.15, cluster extent = 110, small-volume corrected p = .025) and precuneus (peak coordinates: X = 12, Y = -66, Z = 21, T(17) = 5.95, cluster extent = 119, small-volume corrected p = .021), the latter overlapping with the symptom correlated findings, see Fig. 3.

Regarding sgACC connectivity, a significant negative relationship was observed within one cluster in a whole-brain analysis, again located within the posterior precuneus but more dorsally (peak coordinates: X = 0, Y = -72, Z = 24, T(17) = 6.75, cluster extent = 110, cluster-level corrected p = .021), see Fig. 4.

4. Discussion

In this sham-controlled study of iTBS over the dmPFC, we show that the greater the symptom improvement following active iTBS, the greater the increase in connectivity strength between the dmPFC target and a region in the right posterior precuneus. This suggests that successful dmPFC iTBS acts through modulating the targeted dmPFC functional connectivity. One earlier open label study also observed a symptom related change in connectivity with the targeted dmPFC following treatment [18]. Here, we extend this finding in a sham-controlled trial, showing that the connectivity change is specific to active treatment, with precuneus being an important node.

The region within the posterior precuneus showing symptom related connectivity change overlapped with the PCC, a major node in the default mode network (DMN) [37]. A meta-analysis of resting-state connectivity studies in major depression found a decreased connectivity between salience network nodes, including the ACC, and a region similar to ours in the precuneus extending into the PCC and occipital lobe [38]. Thus, one interpretation of the present findings is that the treatment works through strengthening a reduced connectivity between the targeted salience network (SN) and the DMN. A proposed function of the SN is to act as a switch, disengaging the DMN and engaging the central executive network in response to salient events [39]. Consequently, an increased coupling between the SN and DMN may facilitate the regulation of a ruminative state in depression. One needs to keep in mind, however, that we did not directly test for network level connectivity changes in this exploratory seed-based analysis.

Baseline connectivity between the same precuneus/PCC region and the treatment target was also predictive of response to active treatment, when considering blind and open phase treatment together. Similarly, sgACC connectivity to the precuneus at baseline was predictive of

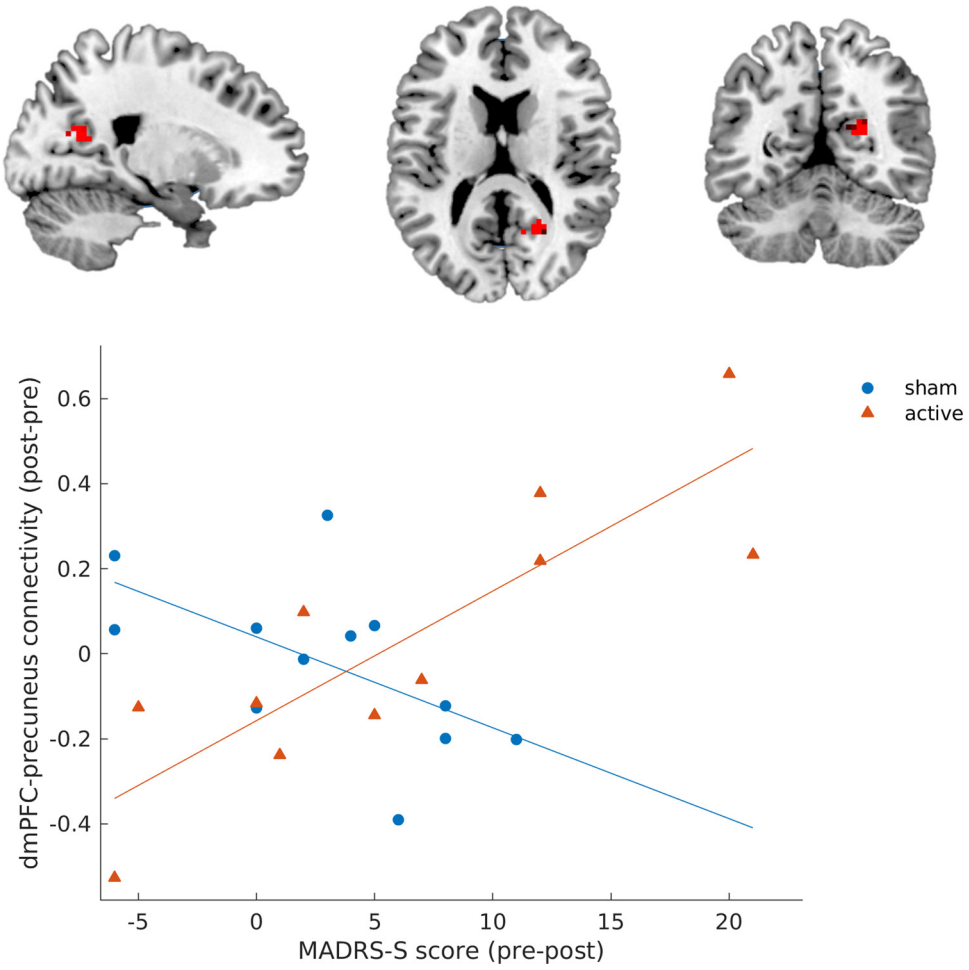

Fig. 2. A) Voxels where increased connectivity with the dorsomedial prefrontal cortex (dmPFC) treatment target was associated with symptom improvement following active compared to sham treatment (peak voxel: X = 21, Y = -60, Z = 21). Orthogonal slices are displayed in neurological convention. B) Scatter plot showing the relationship between connectivity change and symptom change for each group. Note that a positive change in MADRS-S scores corresponds to symptom improvement, while a positive change in connectivity denotes an increased (or reduced negative) connectivity. Testing the relationship in each group separately, only the active group showed a significant relationship between change in connectivity and symptoms.

symptom improvement. This is in line with Salomons et al. (2014) [18] who found both dmPFC and sgACC connectivity with cortical and subcortical regions to be predictive of dmPFC targeted rTMS response. Of note, Drysdale et al. (2017) [40] reported the PCC together with the dmPFC and sgACC as being among the most discriminating connectivity features in responders to dmPFC targeted rTMS. In general, our findings speak to the potential of baseline resting-state connectivity assessments to prioritize or individualize dmPFC targeted iTBS. In the present study, treatment response was fairly low with a large individual variability in symptom change. One possible implication of the results is that individualizing the treatment target based on the connectivity strength between the dmPFC/ACC and the posterior precuneus could be used to improve the response rate.

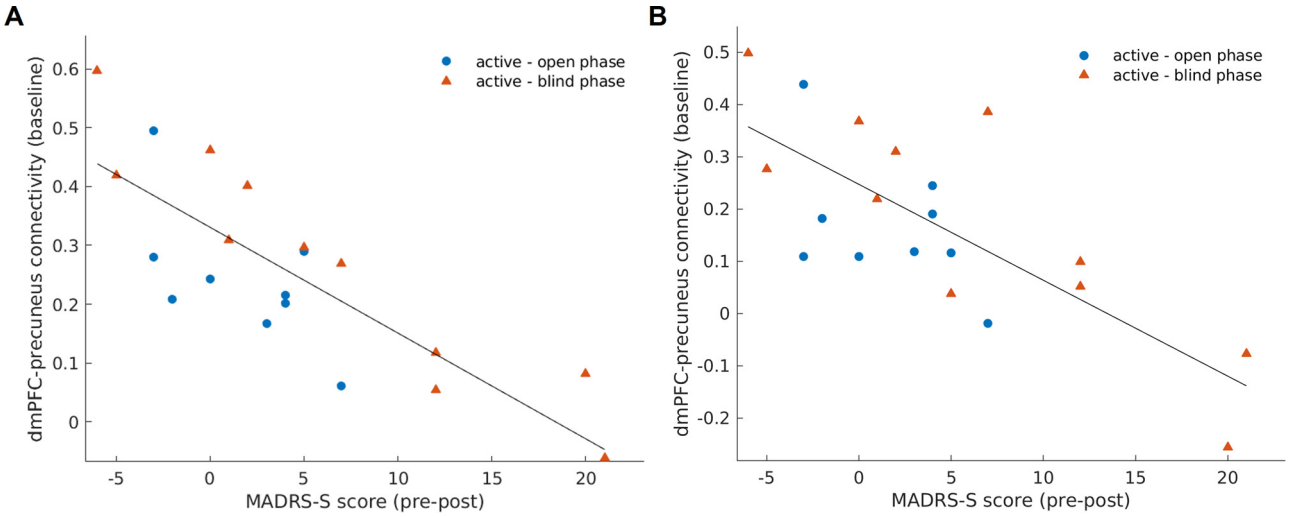

Fig. 3. Baseline connectivity between the treatment target in the dorsomedial prefrontal cortex (dmPFC) and A) the cuneus peak voxel: X = 9, Y = -69, Z = -9) and B) precuneus (peak voxel: X = 12, Y = -66, Z = 21) is negatively correlated with treatment response. The Y axis represents the mean connectivity within the cluster that showed a significant relationship.

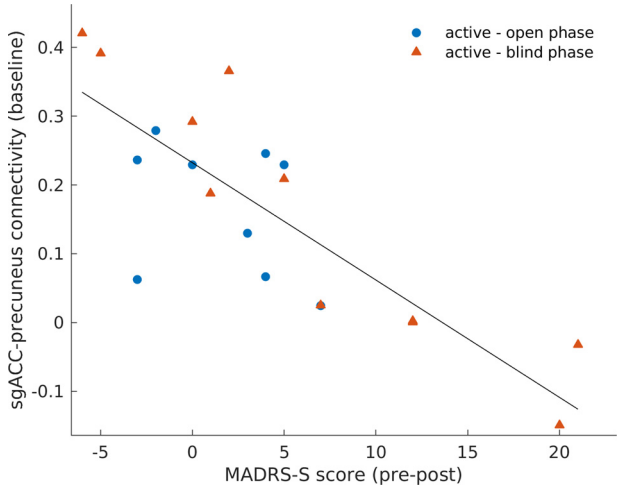

Fig. 4. Baseline connectivity between the subgenual anterior cingulate cortex (sgACC) and the precuneus (peak voxel: X = 0, Y = -72, Z = 24) is negatively correlated with treatment response in a whole-brain analysis. The Y axis represents the mean connectivity within the cluster that showed a significant relationship.

4.1. Limitations

The sample size was relatively small, a problem which was aggravated by data loss due to excessive head movements. This naturally limits the generalizability of the findings. Still, we are able to identify a treatment specific effect and the findings are generally in line with earlier studies as discussed above.

While the treatment targeted a region a few centimeters below the cortical surface, overlapping the dACC, the stimulation likely affected the overlying cortex as well, being more focal closer to the scalp. This leaves open the possibility that the changes in connectivity are indirect, mediated by stimulation of the surface dmPFC. Still, we chose to base the seed region on the targeted coordinates since this was the region of theoretical interest [9,10,31] and since we based the stimulation intensity on the foot, rather than the hand, threshold, targeting a similar depth. Regardless, the findings suggest that the treatment protocol has the potential to modulate the deeper dmPFC/dACC, directly or indirectly.

We did not find a clinical effect of active iTBS over dmPFC compared to sham. This may in part be due to too short a treatment duration. We opted for two daily sessions based on previous findings [4]. However, others have found that more daily sessions, or sessions spaced further apart, are needed to benefit from this approach [5]. Whether iTBS will benefit from accelerated protocols is still an open question for now.

The lack of a clinical effect may also be seen as a limitation with regards to the resting-state connectivity findings. However, behind the lack of an effect is a large individual variability in symptom change. When adding symptom change as a covariate in the connectivity analysis, we ask whether there is a corresponding individual variability in connectivity change. We find that in the active group only, suggesting a specific mechanism for active iTBS. As such, the lack of a clinical effect does not preclude the search for mechanisms that explain the variability in symptom improvement.

The prediction analyses included both blinded and open label treatments. While we controlled for the effect of blinding, this may partly capture placebo response as well [41]. On the other hand, a possible advantage is that the findings may be more generalizable to clinical practice.

5. Conclusions

Here, we observe a treatment specific modulation of dmPFC connectivity following successful iTBS, in a sham controlled study. Only one prior study to our knowledge demonstrate treatment specific modulation of resting state connectivity, and none targeting the dmPFC. As such, the findings have implications for understanding the mechanisms behind rTMS in general and may inform future efforts to individualize the treatment, with precuneus connectivity as a possible predictor of symptom improvement.

CRediT authorship contribution statement

J. Persson: Conceptualization, Methodology, Data curation, Formal analysis, Investigation, Writing - original draft, Funding acquisition. **W. Struckmann:** Investigation, Writing - review & editing. **M. Gingnell:** Conceptualization, Validation, Writing - review & editing. **D. Fällmar:** Validation, Resources, Writing - review & editing. **R. Bodén:** Conceptualization, Supervision, Project administration, Funding acquisition, Writing - review & editing.

Declaration of Competing Interest

The placebo coil was provided to author RB by the manufacturer (MagVenture) as an unrestricted research support. No other authors have any conflicts of interest to disclose.

Acknowledgements

This study was supported by unrestricted grants from the Swedish Society of Medicine, and Märta and Nicke Nasvell Foundation. RB was supported by the Swedish Research Council Grant2016-02362. JP was supported by a postdoctoral grant from the Swedish Brain Foundation.

References

[1] M.T. Berlim, F. van den Eynde, S. Tovar-Perdomo, Z.J. Daskalakis, Response, remission and drop-out rates following high-frequency repetitive transcranial magnetic stimulation (rTMS) for treating major depression: a systematic review and meta-analysis of randomized, double-blind and sham-controlled trials, Psychol. Med. 44 (2014) 225–239, https://doi.org/10.1017/S0033291713000512.

[2] M.T. Berlim, F. Van den Eynde, Z. Jeff Daskalakis, Clinically meaningful efficacy and acceptability of low-frequency repetitive transcranial magnetic stimulation (rTMS) for treating primary major depression: a meta-analysis of randomized, double-blind and sham-controlled trials, Neuropsychopharmacology 38 (2013) 543–551, https://doi.org/10.1038/npp.2012.237.

[3] D.M. Blumberger, F. Vila-Rodriguez, K.E. Thorpe, K. Feffer, Y. Noda, P. Giacobbe, Y. Knyahnytska, S.H. Kennedy, R.W. Lam, Z.J. Daskalakis, J. Downar, Effectiveness of theta burst versus high-frequency repetitive transcranial magnetic stimulation in patients with depression (THREE-D): a randomised non-inferiority trial, Lancet 391 (2018) 1683–1692, https://doi.org/10.1016/S0140-6736(18)30295-2.

[4] N.Y. Tse, M.R. Goldsworthy, M.C. Ridding, J.P. Coxon, P.B. Fitzgerald, A. Fornito, N.C. Rogasch, The effect of stimulation interval on plasticity following repeated blocks of intermittent theta burst stimulation, Sci. Rep. 8 (2018) 8526, https://doi.org/10.1038/s41598-018-26791-w.

[5] C. Nettekoven, L.J. Volz, M. Kutscha, E.-M. Pool, A.K. Rehme, S.B. Eickhoff, G.R. Fink, C. Grefkes, Dose-dependent effects of theta burst rTMS on cortical excitability and resting-state connectivity of the human motor system, J. Neurosci. 34 (2014) 6849–6859, https://doi.org/10.1523/JNEUROSCI.4993-13.2014.

[6] R. Duprat, S. Desmyter, D.R. Rudi, K. van Heeringen, D. Van den Abbeele, H. Tandt, J. Bakic, G. Pourtois, J. Dedoncker, M. Vervaet, S. Van Autreve, G.M.D. Lemmens, C. Baeken, Accelerated intermittent theta burst stimulation treatment in medication-resistant major depression: a fast road to remission? J. Affect. Disord. 200 (2016) 6–14, https://doi.org/10.1016/j.jad.2016.04.015.

[7] N. Bakker, S. Shahab, P. Giacobbe, D.M. Blumberger, Z.J. Daskalakis, S.H. Kennedy, J. Downar, rTMS of the dorsomedial prefrontal cortex for major depression: safety, tolerability, effectiveness, and outcome predictors for 10 Hz versus intermittent theta-burst stimulation, Brain Stimulat. 8 (2015) 208–215, https://doi.org/10.1016/j.brs.2014.11.002.

[8] P.M. Kreuzer, M. Schecklmann, A. Lehner, T.C. Wetter, T.B. Poeppl, R. Rupprecht, D. de Ridder, M. Landgrebe, B. Langguth, The ACDC pilot trial: targeting the anterior cingulate by double cone coil rTMS for the treatment of depression, Brain Stimulat. 8 (2015) 240–246, https://doi.org/10.1016/j.brs.2014.11.014.

[9] J. Downar, Z.J. Daskalakis, New targets for rTMS in Depression: a review of

convergent evidence, Brain Stimulat. 6 (2013) 231–240, https://doi.org/10.1016/j.brs.2012.08.006.
[10] Y.I. Sheline, J.L. Price, Z. Yan, M.A. Mintun, Resting-state functional MRI in depression unmasks increased connectivity between networks via the dorsal nexus, Proc. Natl. Acad. Sci. U. S. A. 107 (2010) 11020–11025, https://doi.org/10.1073/pnas.1000446107.
[11] M. Avissar, F. Powell, I. Ilieva, M. Respino, F.M. Gunning, C. Liston, M.J. Dubin, Functional connectivity of the left DLPFC to striatum predicts treatment response of depression to TMS, Brain Stimulat. 10 (2017) 919–925, https://doi.org/10.1016/j.brs.2017.07.002.
[12] L. Du, H. Liu, W. Du, F. Chao, L. Zhang, K. Wang, C. Huang, Y. Gao, Y. Tang, Stimulated left DLPFC-nucleus accumbens functional connectivity predicts the anti-depression and anti-anxiety effects of rTMS for depression, Transl. Psychiatry 7 (2018) 3, https://doi.org/10.1038/s41398-017-0005-6.
[13] S.J. Iwabuchi, D.P. Auer, S.T. Lankappa, L. Palaniyappan, Baseline effective connectivity predicts response to repetitive transcranial magnetic stimulation in patients with treatment-resistant depression, Eur. Neuropsychopharmacol. (2019), https://doi.org/10.1016/j.euroneuro.2019.02.012.
[14] J. Fan, I.F. Tso, D.F. Maixner, T. Abagis, L. Hernandez-Garcia, S.F. Taylor, Segregation of salience network predicts treatment response of depression to repetitive transcranial magnetic stimulation, Neuroimage Clin. 22 (2019) 101719, , https://doi.org/10.1016/j.nicl.2019.101719.
[15] C. Liston, A.C. Chen, B.D. Zebley, A.T. Drysdale, R. Gordon, B. Leuchter, H.U. Voss, B.J. Casey, A. Etkin, M.J. Dubin, Default mode network mechanisms of transcranial magnetic stimulation in depression, Biol. Psychiatry 76 (2014) 517–526, https://doi.org/10.1016/j.biopsych.2014.01.023.
[16] J.I. Kang, H. Lee, K. Jhung, K.R. Kim, S.K. An, K.-J. Yoon, S.I. Kim, K. Namkoong, E. Lee, Frontostriatal connectivity changes in major depressive disorder after repetitive transcranial magnetic stimulation: a randomized sham-controlled study, J. Clin. Psychiatry 77 (2016) 1137–1143, https://doi.org/10.4088/JCP.15m10110.
[17] J. Downar, J. Geraci, T.V. Salomons, K. Dunlop, S. Wheeler, M.P. McAndrews, N. Bakker, D.M. Blumberger, Z.J. Daskalakis, S.H. Kennedy, A.J. Flint, P. Giacobbe, Anhedonia and reward-circuit connectivity distinguish nonresponders from responders to dorsomedial prefrontal repetitive transcranial magnetic stimulation in major depression, Biol. Psychiatry 76 (2014) 176–185, https://doi.org/10.1016/j.biopsych.2013.10.026.
[18] T.V. Salomons, K. Dunlop, S.H. Kennedy, A. Flint, J. Geraci, P. Giacobbe, J. Downar, Resting-state cortico-thalamic-striatal connectivity predicts response to dorsomedial prefrontal rTMS in major depressive disorder, Neuropsychopharmacology 39 (2014) 488–498, https://doi.org/10.1038/npp.2013.222.
[19] A. Weigand, A. Horn, R. Caballero, D. Cooke, A.P. Stern, S.F. Taylor, D. Press, A. Pascual-Leone, M.D. Fox, Prospective validation that subgenual connectivity predicts antidepressant efficacy of transcranial magnetic stimulation sites, Biol. Psychiatry 0 (2017), https://doi.org/10.1016/j.biopsych.2017.10.028.
[20] S.F. Taylor, S.S. Ho, T. Abagis, M. Angstadt, D.F. Maixner, R.C. Welsh, L. Hernandez-Garcia, Changes in brain connectivity during a sham-controlled, transcranial magnetic stimulation trial for depression, J. Affect. Disord. 232 (2018) 143–151, https://doi.org/10.1016/j.jad.2018.02.019.
[21] M. Tik, A. Hoffmann, R. Sladky, L. Tomova, A. Hummer, L. Navarro de Lara, H. Bukowski, J. Pripfl, B. Biswal, C. Lamm, C. Windischberger, Towards understanding rTMS mechanism of action: stimulation of the DLPFC causes network-specific increase in functional connectivity, NeuroImage 162 (2017) 289–296, https://doi.org/10.1016/j.neuroimage.2017.09.022.
[22] I. Hadas, Y. Sun, P. Lioumis, R. Zomorrodi, B. Jones, D. Voineskos, J. Downar, P.B. Fitzgerald, D.M. Blumberger, Z.J. Daskalakis, Association of repetitive transcranial magnetic stimulation treatment with subgenual cingulate hyperactivity in patients with major depressive disorder: a secondary analysis of a randomized clinical trial, JAMA Netw. Open 2 (2019) e195578, https://doi.org/10.1001/jamanetworkopen.2019.5578.
[23] D.V. Sheehan, Y. Lecrubier, K.H. Sheehan, P. Amorim, J. Janavs, E. Weiller, T. Hergueta, R. Baker, G.C. Dunbar, The Mini-International Neuropsychiatric Interview (M.I.N.I): the development and validation of a structured diagnostic psychiatric interview for DSM-IV and ICD-10, J. Clin. Psychiatry 59 (1998) 22–33.
[24] J.O. Brooks, J.C. Bonner, A.C. Rosen, P.W. Wang, J.C. Hoblyn, S.J. Hill, T.A. Ketter, Dorsolateral and dorsomedial prefrontal gray matter density changes associated with bipolar depression, Psychiatry Res. Neuroimaging 172 (2009) 200–204, https://doi.org/10.1016/j.pscychresns.2008.06.007.
[25] J.O. Brooks, P.W. Wang, J.C. Bonner, A.C. Rosen, J.C. Hoblyn, S.J. Hill, T.A. Ketter, Decreased prefrontal, anterior cingulate, insula, and ventral striatal metabolism in medication-free depressed outpatients with bipolar disorder, J. Psychiatry Res. 43 (2009) 181–188, https://doi.org/10.1016/j.jpsychires.2008.04.015.
[26] M. Mula, S. Pini, S. Calugi, M. Preve, M. Masini, I. Giovannini, P. Rucci, G.B. Cassano, Distinguishing affective depersonalization from anhedonia in major depression and bipolar disorder, Compr. Psychiatry 51 (2010) 187–192, https://doi.org/10.1016/j.comppsych.2009.03.009.
[27] M. Di Nicola, L. De Risio, C. Battaglia, G. Camardese, D. Tedeschi, M. Mazza, G. Martinotti, G. Pozzi, C. Niolu, M. Di Giannantonio, A. Siracusano, L. Janiri, Reduced hedonic capacity in euthymic bipolar subjects: a trait-like feature? J. Affect. Disord. 147 (2013) 446–450, https://doi.org/10.1016/j.jad.2012.10.004.
[28] Q. Ma, Y. Tang, F. Wang, X. Liao, X. Jiang, S. Wei, A. Mechelli, Y. He, M. Xia, Transdiagnostic dysfunctions in brain modules across patients with schizophrenia, bipolar disorder, and major depressive disorder: a connectome-based study, Schizophr. Bull. 46 (2020) 699–712, https://doi.org/10.1093/schbul/sbz111.
[29] J.T. Baker, D.G. Dillon, L.M. Patrick, J.L. Roffman, R.O. Brady, D.A. Pizzagalli, D. Öngür, A.J. Holmes, Functional connectomics of affective and psychotic pathology, Proc. Natl. Acad. Sci. 116 (2019) 9050–9059, https://doi.org/10.1073/pnas.1820780116.
[30] S.A. Montgomery, M. Åsberg, A new depression scale designed to be sensitive to change, Br. J. Psychiatry 134 (1979) 382–389, https://doi.org/10.1192/bjp.134.4.382.
[31] A. Mir-Moghtadaei, P. Giacobbe, Z.J. Daskalakis, D.M. Blumberger, J. Downar, Validation of a 25% nasion–inion heuristic for locating the dorsomedial prefrontal cortex for repetitive transcranial magnetic stimulation, Brain Stimulat. 9 (2016) 793–795, https://doi.org/10.1016/j.brs.2016.05.010.
[32] C.-G. Yan, X.-D. Wang, X.-N. Zuo, Y.-F. Zang, DPABI: data processing & analysis for (Resting-State) brain imaging, Neuroinformatics 14 (2016) 339–351, https://doi.org/10.1007/s12021-016-9299-4.
[33] K.J. Friston, S. Williams, R. Howard, R.S.J. Frackowiak, R. Turner, Movement-related effects in fMRI time-series, Magn. Reson. Med. 35 (1996) 346–355, https://doi.org/10.1002/mrm.1910350312.
[34] M. Jenkinson, P. Bannister, M. Brady, S. Smith, Improved optimization for the robust and accurate linear registration and motion correction of brain images, NeuroImage 17 (2002) 825–841, https://doi.org/10.1006/nimg.2002.1132.
[35] L. Parkes, B. Fulcher, M. Yücel, A. Fornito, An evaluation of the efficacy, reliability, and sensitivity of motion correction strategies for resting-state functional MRI, NeuroImage 171 (2018) 415–436, https://doi.org/10.1016/j.neuroimage.2017.12.073.
[36] T.E. Nichols, A.P. Holmes, Nonparametric permutation tests for functional neuroimaging: a primer with examples, Hum. Brain Mapp. 15 (2002) 1–25, https://doi.org/10.1002/hbm.1058.
[37] R.L. Buckner, J.R. Andrews-Hanna, D.L. Schacter, The brain's default network, Ann. N. Y. Acad. Sci. 1124 (2008) 1–38, https://doi.org/10.1196/annals.1440.011.
[38] R.H. Kaiser, J.R. Andrews-Hanna, T.D. Wager, D.A. Pizzagalli, Large-scale network dysfunction in major depressive disorder: a meta-analysis of resting-state functional connectivity, JAMA Psychiatry 72 (2015) 603–611, https://doi.org/10.1001/jamapsychiatry.2015.0071.
[39] V. Menon, L.Q. Uddin, Saliency, switching, attention and control: a network model of insula function, Brain Struct. Funct. 214 (2010) 655–667, https://doi.org/10.1007/s00429-010-0262-0.
[40] A.T. Drysdale, L. Grosenick, J. Downar, K. Dunlop, F. Mansouri, Y. Meng, R.N. Fetcho, B. Zebley, D.J. Oathes, A. Etkin, A.F. Schatzberg, K. Sudheimer, J. Keller, H.S. Mayberg, F.M. Gunning, G.S. Alexopoulos, M.D. Fox, A. Pascual-Leone, H.U. Voss, B.J. Casey, M.J. Dubin, C. Liston, Resting-state connectivity biomarkers define neurophysiological subtypes of depression, Nat. Med. 23 (2017) 28–38, https://doi.org/10.1038/nm.4246.
[41] G.-R. Wu, X. Wang, C. Baeken, Baseline functional connectivity may predict placebo responses to accelerated rTMS treatment in major depression, Hum. Brain Mapp. (2019), https://doi.org/10.1002/hbm.24828.